A New All-Atom Force Field for Crystalline Cellulose I

S. NEYERTZ,[1] A. PIZZI,[2] A. MERLIN,[3] B. MAIGRET,[4] D. BROWN,[1] X. DEGLISE[3]

[1] Laboratoire des Matériaux Polymères et Composites, UMR CNRS 5041, Bât. IUT, Savoie Technolac, 73776 Le Bourget-du-Lac, France

[2] ENSTIB, Université de Nancy I, BP 1041, 88051 Epinal Cedex, France

[3] Laboratoire de Photochimie Appliquée, Université de Nancy I, BP 239, 54506 Vandoeuvre-lès-Nancy, France

[4] Laboratoire de Chimie Théorique, UMR CNRS 7565, Université de Nancy I, BP 239, 54506 Vandoeuvre-lès-Nancy Cedex, France

Received 22 March 1999; accepted 25 January 2000

ABSTRACT: The details of a new all-atom force field designed to reproduce the phases of the native I-α and I-β forms found in crystalline cellulose I are reported in this article. The energy differences, densities, unit cell parameters, and moduli are in close agreement with experimental evidence. Analyses of the modular dynamics simulations also included thermodynamic data and angle distributions as well as characterization of the intrachain, intrasheet, and intersheet hydrogen-bond networks for both phases under study. © 2000 John Wiley & Sons, Inc. J Appl Polym Sci 78: 1939–1946, 2000

Key words: cellulose; force field; molecular dynamics; crystal structure; hydrogen-bond network

INTRODUCTION

The crystal structure of cellulose has been the subject of investigations for many decades, and a number of conflicting models have been proposed.[1–5] A breakthrough came in the mid-1980s when it was established by solid-state ^{13}C nuclear magnetic resonance that native crystalline cellulose is actually a composite of two distinct forms, a triclinic parallel-packed cellulose, I-α, and a monoclinic parallel-packed phase cellulose, I-β, with the I-α/I-β ratio depending on its origin.[6,7]

Computer simulation can be used as a complement to experimental studies by providing information at the atomistic level. Molecular dynamics (MD) simulations[8] solve the equations of motion for all the atoms in a system and thus provide direct dynamic information in addition to data on static properties. To date, MD simulations have been carried out on the crystalline celluloses I-α and I-β using the CHARMM force field,[9] which led to the conclusion that the strength of hydrogen-bonding and hydrophobic interactions was underestimated in the parameter set. Another study[10] was conducted with a parameter set for carbohydrates[11] based on the CHARMM22 force field. The elastic modulus of cellulose I and the cell parameters for the monoclinic I-β phase were found to be in good agreement with the experimental data[12]; however, deviations of as much as 10° for the γ angle of the triclinic I-α phase were reported. Two groups[13–15] have reported the results of MD simulations using the united-atom GROMOS force field for carbohydrates.[16]

Correspondence to: A. Pizzi.

Journal of Applied Polymer Science, Vol. 78, 1939–1946 (2000)

According to Heiner et al.,[13] who used constant volume simulations, it was discovered that the main drawbacks of the force field were a large positive total energy and a large negative pressure (−5800 bars for I-β). However, they did not change the shape and size of their electron-diffraction-based monoclinic unit cell[17] to quantify the distortion of the cell required to return atmospheric pressure, and for computational reasons they did not monitor the pressure in the triclinic system.[13] Kroon-Batenburg et al.[14,15] simulated cellulose I and II with the same force field, at both constant volume and constant pressure. These authors overcame the restriction of the GROMOS program by transforming the triclinic I-α cell into an equivalent monoclinic form.[14] Their final constant-pressure unit cell parameters were very close to those of an earlier study by Gardner and Blackwell,[4] although this latter structure was later discarded by the same group[15] because of a preference for that of Sarko and Muggli.[3] However, it is worth noting that good agreement has been reported for the ^{13}C-NMR chemical shifts using this united-atom force field.[18]

In this article we present details of a new, fully atomistic MD potential model for cellulose that attempts to overcome the shortcomings mentioned above. Results from constant-pressure MD simulations of the crystalline phase of both celluloses I-α and I-β show that the new model performs well. As our ultimate aim is to create a model of the cellulose–PEO interface, we have carried out the present work within the framework of a potential model previously published for PEO.[19] We have also adopted a specific approach to force-field development by optimizing our parameters with respect to a given system rather than using a consistent force-field approach, in which a range of systems can be reasonably modeled but often at the cost that one will not be reproduced particularly well. Since we were interested in a specific crystalline cellulose-based system, we chose the alternative of starting with infinitely long chains, for which there is good reason to assume that all monomers can be treated as equivalent. Thus, the work presented in this article was initially restricted to cellulose only, but we believe that the specific models are justified by the numerous applications of this molecule, of which the cellulose–PEO interface is only one example. Different full-atom parameter sets for cellulose have been screened in a series of short MD simulations, and an optimized force field has been chosen.

EXPERIMENTAL

The Cellulose Model

Analytical Form of the Force Field

The potential energy of the cellulose model is described in terms of "bonded" angle bending and torsional interactions arising from near-neighbor connections in the structure, as well as "nonbonded" van der Waals and electrostatic interactions, depending on the distance between atoms. Atoms belonging to the same molecule but separated by more than three bonds, as well as atoms belonging to different molecules, interact through the "nonbonded" potentials.

The analytical form of the potential is in keeping with that described before for PEO.[19] We distinguish five basic atom types for cellulose: (1) carbons, C; (2) hydrogens bonded to carbons, H; (3) hydroxyl oxygens, O(H); (4) hydroxyl hydrogens, H(O); and (5) ether oxygens, O(eth). All bond lengths are rigidly constrained to 1.516 Å for C—C, 1.420 Å for C—O(H), 1.445 Å for C—O(eth), 1.111 Å for C—H, and 0.960 Å for O(H)—H(O) bonds.[11]

Such a potential probably represents the simplest all-atom model that can be expected to give reasonable results. Although a more detailed model might include, for example, anomeric effects[20] or explicit hydrogen-bonding potentials, these introduce many more parameters into an already complicated calculation. Indeed, hydrogen bonds can form through a combination of "nonbonded" excluded-volume and electrostatic potentials.[21]

Starting Structures

The initial structures for crystalline I-α and I-β cellulose were based on the reported parameters obtained from the electron diffraction study of *Microdictyon tenuius* cellulose[17] and a synchrotron diffraction study.[22] Cellulose I-α has a one-cellobiose P1 triclinic unit cell, with a = 6.74 Å, b = 5.93 Å, c (chain axis) = 10.36 Å, α = 117°, β = 113°, γ = 81°. Cellulose I-β has a two-cellobiose $P2_1$ monoclinic unit cell, with a = 7.85 Å, b = 8.25 Å, c (chain axis) = 10.36 Å, α = 90°, β = 90°, γ = 96.66°. The structure and the nomenclature of

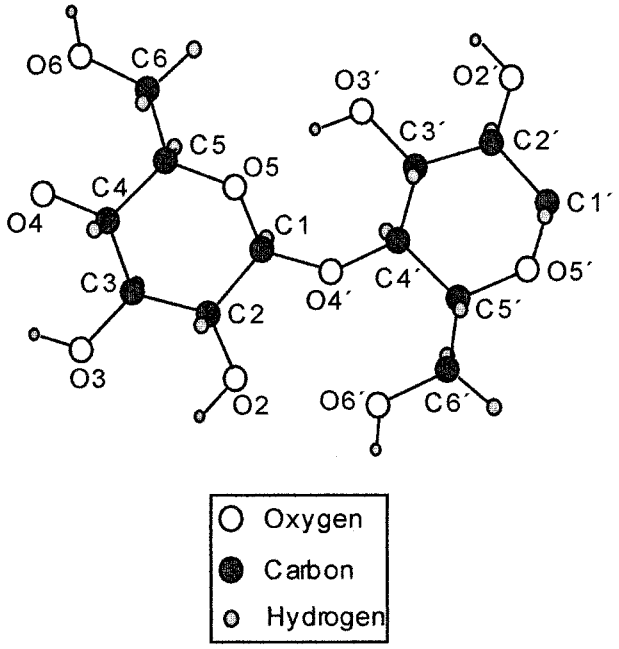

Figure 1 Structure and nomenclature of cellulose. Note that O4 is linked to a C1′. Hydrogens carried by C*n* will be referred to in the text as H*n*, while hydrogens carried by O*n* will be referred to as HO*n*.

a cellulose chain are given in Figure 1. Atoms are designated by their indices on the chain with C*n* being the *n*th carbon, O*n* the *n*th oxygen, H*n* the hydrogen bonded to the *n*th carbon, and HO*n* the hydrogen bonded to the *n*th oxygen.

The crystallographic I-α and I-β unit cells were replicated through space to build periodic MD (3∞3∞2) and (3∞2∞2) supercells, respectively. The crystalline I-α cellulose simulation box contained 756 atoms in 9 effectively infinite chains, while the cellulose I-β simulation box contained 1008 atoms in 12 effectively infinite chains.

Potential Optimization

The parameters used in the potential model may be derived from various standard or specific sources. However, it has been argued that one of the main limitations of standard parameterizations is the lack of accurate torsional potentials for these molecules.[23] Therefore, we have only considered parameter sets that were either developed for organic molecules or specifically designed for carbohydrates.[11,23–26]

Initial test MD simulations were carried out for the 756-atom system of crystalline cellulose I-α at a temperature of 300 K because the different angles in the triclinic structure allow for a more fine-tuned screening than monoclinic cellulose I-β. Unlike the GROMOS MD simulations,[13–15] our pressure calculation scheme[27] can be used directly for boxes of arbitrary size and shape. All simulations reported here were performed using the *gmq* program.[28] Computational details have been given previously.[19] A series of test simulations was run under NPT constant pressure conditions up to 200 ps and results were averaged over the last 50 ps of each run, by which time the systems were well equilibrated.

The average density (ρ), scalar pressure (p), pressure tensor components ($P\alpha\beta$), and crystallographic cell parameters (a), (b), (c), (α), (β) and (γ) of crystalline cellulose I-α were studied for each parameter combination under study. The best results were obtained for a combination of (1) bending potentials derived from[11,24,25]; (2) torsional potentials obtained from *ab initio* calculations of fragment carbohydrate molecules at the MP2/6-311+G(2d,2p)// 6-31G** level and at CHARMM22[11]; (3) excluded-volume parameters calculated from the universal force field (UFF)[29]; and (4) charges obtained by Ha et al. for α-D-glucopyranose,[26] with slight changes to maintain the electroneutrality of the systems. The experimentally determined density, 1586.1 kg m^{-3},[17] differed from the average relaxed MD density, 1559.6 kg m^{-3}, by less than ~1.7%. Cell lengths were modified by up to ~0.21 Å for a, ~0.13 Å for b, and ~0.07 Å for c. The changes in angles were on the order of ~0.1° for α, ~0.4° for β, and ~2.2° for γ. All parameters for this optimized combination are given in Tables I–IV.

Table I Parameters for Intramolecular Bending Potentials

Bending Potential $V_{\text{bend}}(\theta) = \frac{k_\theta}{2}(\cos\theta - \cos\theta_0)^2$

Bond-angle	θ_0	k_θ
C—C—C	111.00	91.7881
C—C—O(H)	110.10	113.3918
C—C—O(eth)	105.00	107.1797
H—C—C	110.10	79.3743
H—C—H	109.00	78.2993
H—C—O(H)	108.89	78.1962
H—C—O(eth)	107.24	76.7408
O(eth)—C—O(eth)	111.55	214.0840
H(O)—O—C	106.00	119.0445
C—O(eth)—C	107.50	131.9296

[a] θ_0 are given in degrees and k_θ in kcal mol^{-1}.

Table II Parameters for Intramolecular Torsional Potential[a]

Torsional Potential $V_{tors}(\tau) = \sum_{n=0}^{4} a_n \cos^n \tau$

Torsion Angle	a_0	a_1	a_3
O(H)—C—C—O(H)	−1.63	2.83	−1.20
O(H)—C—C—O(eth)	−1.84	3.04	−1.20
C—C—O(eth)—C	0.60	0.00	−0.60
C—C—C—O(H)	0.83	−0.23	−0.60
C—O(eth)—C—O(eth)	−1.15	1.95	−0.80
X—C—C—X	0.15	0.45	−0.60
X—C—O(eth)—X	0.10	0.30	−0.40
X—C—O(H)—H(O)	0.14	0.42	−0.56

[a] The sets of coefficients, a_i for $i = 0$, 1, and 3, are given in kcal mol^{-1}. a_2 is always equal to 0. X refers to atoms for which the corresponding torsional potential has not been explicitly defined elsewhere in the table.

MD Production Runs

NPT production runs were carried out over 350 ps with optimized potential for both crystalline cellulose I-α and I-β. The average magnitude of the mean square displacement vectors between the minimized-energy and the room-temperature structures is 0.38 Å for cellulose I-α and 0.32 Å for cellulose I-β, which is very small in MD terms. These plateau values are attained very quickly and show no sign of diffusive-type behavior, thus indicating that the systems remained crystalline over the length of the simulations. A postanalysis was then conducted over the last 200 ps of each run. A schematic representation of the MD cell at the end of both production runs is given in Figure 2(a,b). A series of 150-ps NPT simulations was also carried out with a rate of change of the externally applied pressure component along the chain axis, P_{zz}, set to −200 bars/ps. The elongations of the chains were subsequently recorded in order to calculate the Young's moduli of crystalline cellulose I-α and I-β.

RESULTS AND DISCUSSION

In their MD study of crystalline cellulose based on unrefined coordinates obtained by electron diffraction, Heiner et al. draw a distinction between chains in the odd and those in the even (200) crystalline I-β planes, indicating two close but nonequivalent chain structures in the monoclinic system.[13] We conduct here our analysis of the cellulose I-β phase without making any *a priori* assignments of odd and even planes.

Thermodynamic Data

Thermodynamic properties of the relaxed systems were obtained for both cellulose I-α and I-β from the production runs. Average density, pressure, and cell shape for cellulose I-α is identical to those reported for the optimized test simulation described above, although statistics were improved because of the longer simulation times. The average density for cellulose I-β, 1612.5 kg m^{-3}, lies within 0.25% of the experimentally determined density, 1616.1 kg m^{-3}.[22] Deviations from the experimental cellulose I-β cell shape[22] were on the order of ~0.28 Å for *a,* ~0.31 Å for *b,* ~0.02 Å for *c,* ~0.05° for α, ~0.02° for β, and ~0.63° for γ. The potential model, optimized for cellulose I-α, is thus also in very good agreement with the experiment for cellulose I-β.

The total energies (U) suggest that cellulose I-β ($U = -201.38$ kcal mol^{-1} of cellobiose) is thermodynamically more stable than cellulose Iα ($U = -199.54$ kcal mol^{-1} of cellobiose), in accord with hydrothermal annealing results.[30,31] The total energy difference, $[U(\text{I-}\beta)] - [U(\text{I-}\alpha)]$, is −1.84 kcal mol^{-1} of cellobiose, which corresponds to

Table III Partial Charges, q_i/e for the Electrostatic Potential

Electrostatic Potential $V_{coul}(|r_{ij}|) = \frac{q_i q_j}{4\pi\varepsilon_0 |r_{ij}|}$

Atoms	C1	C2 C3 C4	C5	C6	O2 O3 O6	O4	O5	All H Attached to C	All H Attached to O
Charges	0.350	0.150	0.100	0.050	−0.650	−0.500	−0.400	0.100	0.400

Table IV Parameters for Buckingham Potential[a]

Buckingham Potential $V_{\text{Buck}}(|r_{ij}|) = D \exp\left(-\frac{|r_{ij}|}{\rho}\right) - \frac{E}{|r_{ij}|^6}$

Atom Pair	D	ρ	E
O(H)···O(H), O(H)···O(eth), O(eth)···O(eth)	58298.9	0.2485	192.1
O(H)···C, O(eth)···C	42931.6	0.2755	352.8
O(H)···H, O(eth)···H, O(H)···H(O), O(eth)···H(O)	20432.6	0.2445	98.8
C···C	31615.1	0.3025	647.8
C···H, C···H(O)	15046.7	0.2715	181.5
H···H, H···H(O), H(O)···H(O)	7161.2	0.2405	50.8

[a] D is given in kcal mol^{-1}, ρ in Å, and E in kcal mol^{-1} Å^6.

-7.70 kJ mol^{-1} of cellobiose. In agreement with Heiner et al.,[13] the main contribution to the energy and the energy difference between both forms of native cellulose results from the electrostatic interactions, with cellulose I-β slightly favored.

Angle Distributions

Probability density distributions were calculated for both bending and torsional angles over the cellulose I-α and I-β production runs. The glycosidic linkage average angle was found to be more open in the I-α phase (112.0°) than in the I-β (111.5°) phase, which resulted in marginally more extended I-α than I-β chains. Torsion angles around the ring backbones remained in their initial wells. Using the convention where τ is *gauche*$-$ (g^-) if $180° \leq \tau \leq -60°$, *trans* (t) if $-60° < \tau < 60°$, and *gauche*$+$ (g^+) if $60° \leq \tau \leq 180°$, both I-α and I-β rings retain a $g^- - g^+ - g^- - g^+ - g^- - g^+$ conformation, starting clockwise from the C1—C2—C3—C4 angle.

According to the convention of Blackwell et al.,[32] the conformation of the —CH_2OH side groups can be denoted as gt, tg or gg, where the first state stands for the O5—C5—C6—O6 torsion and the second state for the C4—C5—C6—O6 torsion; only three possibilities exist, as these two angles must differ by 120°. Our results suggest a gt arrangement. The same result was obtained by analyzing energy-minimized configurations. It is worth noting that two distinct peaks appeared in the density functions for cellulose I-β. The system spontaneously evolved toward the alternating layers structure of cellulose I-β, suggested by Heiner et al.[13] Indeed, these authors indicate a shift of ~26° between the experimental value of ω in their Iβ/odd and Iβ/even planes, while the difference between both peaks was ~25°. The alternating layers are also apparent in Figure 2(b).

According to Blackwell et al.,[32] the hydroxymethyl groups adopt gt and gg positions, with a predominance of the former for both cellulose I-α and I-β. The results of calculations with the GROMOS and MM3 force fields have shown that a tg conformation is favored for these —CH_2—OH groups.[13–15,33] In contrast to the above, high-temperature annealing simulations, designed to cross energy barriers and better explore the conformational space,[10–12] have led to the conclusion that minimum energy conformation in cellulose is indeed a gt conformer. Further supporting evidence comes from the observability of gt and gg geometries in hexose monomers, dimers, and polysaccharide chains,[32,33] unlike their tg counterpart, and the belief that the hydroxymethyl groups in cellulose II, easily obtained from cellulose I, are also in the gt position.[10,15]

Hydrogen Bonding

Hydrogen bonds (H-bonds) were found to form from a combination of the excluded-volume and electrostatic potentials. Indeed, peaks appear in several distance distribution functions for On—HOn ··· Om interactions (n = 2, 3, 6; m = 2, 3, 4, 5, 6; please note that there is no distinction between On and On' or Om and Om' (Fig. 1) at values smaller than 3.195 Å, which corresponds to the sum of the van der Waals radii for an oxygen and an hydrogen in the UFF force field.[29] Our choice of a hydrogen-bond criterion was less

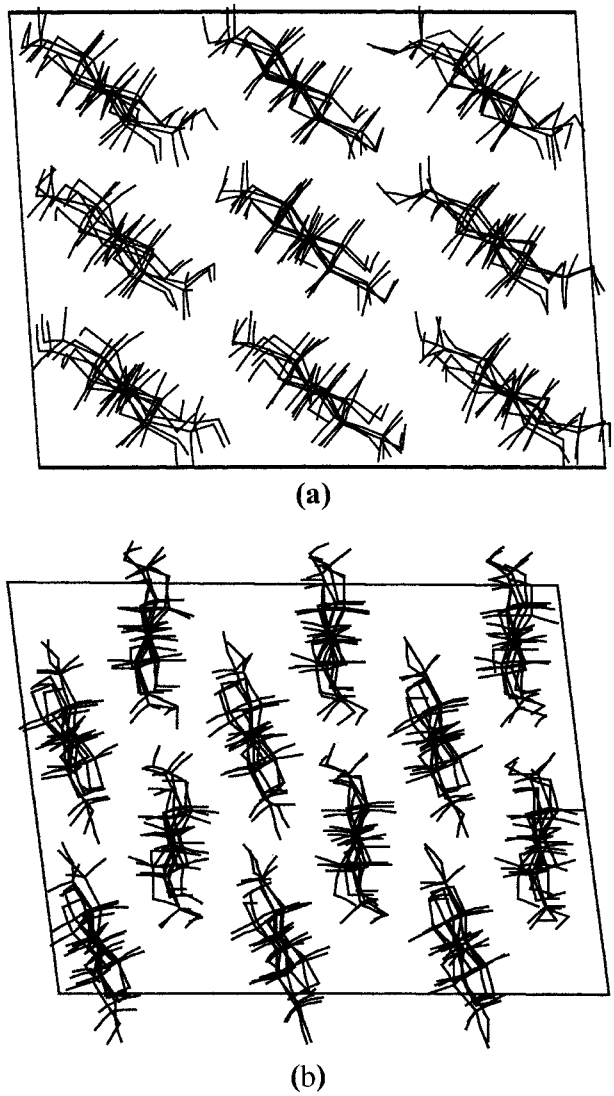

Figure 2 Schematic views down the chain axis of the crystalline MD cell at the end of the 200-ps production run at $T = 300$ K and $p \sim 1$ bar for (a) cellulose I-α and (b) cellulose I-β.

restrictive than that of others,[13,15] but it allowed us to assess the totality of the structural features appearing at distances inferior to the sum of the van der Waals radii for the relevant atoms. The contribution of intrachain, intrasheet, or intersheet interactions to each H-bond type was then determined. Both phases show a slightly different hydrogen-bonding pattern, which is in agreement with IR and Raman spectra studies showing different absorption peaks in the OH stretching and bending regions[34,35] in cellulose Iα and Iβ.

Intrachain H-bonds form through identical interactions. The strongest intrachain H-bond donor is O3, which stabilizes the chain by coordinating to the nearest glycosidic (O4), backbone ether (O5), and, to a lesser extent, hydroxymethyl (O6) oxygens on the neighboring ring in cellulose I-α. On the other hand, there is more competition between these three types of hydrogen bonds in cellulose I-β, thus resulting in three similar distribution peaks. O2 is also a strong donor in cellulose I-α, where its hydrogen interacts with the neighboring O3 on the same ring. Steric interactions limit the formation of this H-bond in cellulose I-β, presumably because of the less open character of its ring structures. O6 only acts as an intrachain hydrogen-bond donor when coordinating to its backbone ring's O5 ether oxygen. In addition, both MD studies that were done with the GROMOS force field report the strength of O2 and O3 as intrachain hydrogen donors.[13,15] The main discrepancies with our simulations are their slightly different hydrogen-bond criteria and the strong O2—HO2 $\cdots$ O6 H-bond, which agrees with their initial tg conformation for —CH_2—OH groups.[13,15] Our gt conformation resulted in the O3—HO3 $\cdots$ O6 H-bond instead, but this confirms the position of O6 as a strong acceptor.

Intrasheet hydrogen bonding shows formation of O2—HO2 $\cdots$ O6 and O6—HO6 $\cdots$ O2 H-bonds; that is, O2 and O6 act both as donors and as acceptors. Cellulose I-α chains are held together in a plane by both types of H-bonds in similar proportions. On the other hand, cellulose I-β chains seem to be mostly coordinated via shorter O6—HO6 $\cdots$ O2 H-bonds. Other MD studies confirm this picture of the intrasheet donor carrying an —OH group and the acceptor belonging to the —CH_2—OH group or vice-versa.[10,13,15]

Unlike intrachain and intrasheet H-bonds, different interactions are at the basis of intersheet hydrogen bonding for cellulose I-α and I-β. O2, O3, and O6 are all strong hydrogen donors in the I-α phase, where they mostly form O2—HO2 $\cdots$ O4, O2—HO2 $\cdots$ O6, O3—HO3 $\cdots$ 06, and O6—HO6 $\cdots$ O4 H-bonds. Although O2—HO2 $\cdots$ O6, O3—HO3 $\cdots$ O6, and O6—HO6 $\cdots$ O4 H-bonds remain important in the I-β phases, two new interactions appear: O2—HO2 $\cdots$ O3 and O3—HO3 $\cdots$ O5. Since the donor and acceptor groups do not have the flexibility of the hydroxymethyl, they show the stronger intercohesion of I-β sheets, which is related to their lower energy. Neither Kroon-Batenburg et al.[15] nor Reiling et al.[10] have reported any three-dimensional inter-

sheet H-bonding in their optimized systems. Heiner et al. found intersheet H-bonds, with O6 acting mostly as a donor or as an acceptor in the triclinic phase; this is in agreement with our findings. They also got O2—HO2 $\cdots$ O3 interactions in the monoclinic phase.[13]

Modulus

To investigate the mechanical properties of our model, the equilibrated configurations of cellulose I-α and I-β at 300 K were subjected to a gradually increasing uniaxial tension along the chain axis by changing the z component of the applied tensor pressure ($P^{0,zz}$) at a constant rate of 200 bar/ps. The response of the **h** matrix, defining the size and shape of the primary cell, and the internal pressure tensor (**P**) were monitored. At low strains, for a system with a well-defined Young's modulus (E), the measured tension ($-P_{zz}$) is related to the extension $_{\gamma L}$ by $-P_{zz} = E_{\gamma L}$. More details can be found about the computational method elsewhere.[36] With up to the 2% extensions applied, the tension obtained is linear and gave Young's moduli of 127.8 GPa for cellulose I-α and 115.2 GPa for cellulose I-β at room temperature. If we consider the I-α/I-β ratio in cellulose I to be 0.65/0.35,[7] the weighted-average Young's modulus for cellulose I is 123.4 GPa with our model. This values fall within the 120–140 GPa range for the crystallite modulus of native cellulose, as measured by X-ray diffraction,[37] which was found to be highly dependent on intrachain hydrogen bonding.[38]

CONCLUSIONS

As shown by the above analyses, our fully atom-optimized model reproduces well the crystalline structures of both cellulose I-α and I-β. Indeed, the constant-pressure NPT simulations of the triclinic and monoclinic phases have allowed for finely tuned parameter screening. The total energy is negative, as should be expected from room-temperature unstrained crystals, with cellulose I-β being slightly more stable than cellulose I-α. Systems relax spontaneously toward experimental densities and cell shapes. The gt conformation of the hydroxymethyl group shows it is fully compatible with crystalline cellulose I, while its intrachain, intrasheet, and interchain hydrogen-bond networks reflect its strong stability. The Young's moduli also fall within the experimental range. Since the model presented here has been developed within the framework of a specific force-field approach for infinitely long-chain cellulose, we have reservations about its use for shorter oligomers where end effects are likely to be significant. However, the results are a promising basis for extending these simulations to other cellulose crystals, as well as to mixed phases such as cellulose–PEO interfaces. It can reasonably be used to describe the cellulose–cellulose interactions in these systems, while being combined with additional interactions when other components are added to the pure cellulose phase.

REFERENCES

1. Mark, H.; Meyer, K. H. Ber Deutsch Chem Ges 1928, 61B, 593.
2. Meyer, K. H.; Misch, L. Helv Chim Acta 1937, 11, 534.
3. Sarko, A.; Muggli, R. Macromolecules 1974, 7, 486.
4. Gardner, K. H.; Blackwell, J Biopolymers 1974, 13, 1975.
5. Woodcock, C.; Sarko, A. Macromolecules 1980, 13, 1183.
6. Atalla, R. H.; van der Hart, D. L. Science 1984, 223, 283.
7. van der Hart, D. L.; Atalla, R. H. Macromolecules 1984, 17, 1465.
8. Allen, M. P.; Tildesley, D. J. Computer Simulation of Liquids; Clarendon Press: Oxford, 1987.
9. Hardy, B. J.; Sarko, A. Polymer 1996, 37, 1833.
10. Reiling, S.; Brickmann, J Macromol Theory Simul 1995, 4, 725.
11. Reiling, S.; Schlenkrich, M.; Brickmann, J. J Comput Chem 1996, 17, 450.
12. Marhöfer, R. J.; Reiling, S.; Brickmann, J Ber Bunsenges Phys Chem 1996, 100, 1350.
13. Heiner, A. P.; Sugiyama, J.; Teleman, O. Carbohydr Res 1995, 273, 207.
14. Kroon-Batenburg, L. M. J.; Bouma, B.; Kroon, J Macromolecules 1996, 29, 5695.
15. Kroon-Batenburg, L. M. J.; Kroon, J. Glycoconjugate J 1997, 14, 677.
16. Koehler, J.; Saenger, W.; v. Gunsteren, W. F. Eur Biophys J 1987, 15, 197.
17. Sugiyama, J.; Vuong, R.; Chanzy, H. Macromolecules 1991, 24, 4168.
18. Heiner, A. P.; Teleman, O. Pure Appl Chem 1996, 68, 2187.
19. Neyertz, S.; Brown, D. J. Chem Phys 1995, 102, 9725.
20. Tvaroska, I.; Bleha, T. Adv Carbohydr Chem Biochem 1989, 47, 45.

21. Israelachvili, J. Intermolecular & Surface Forces; Academic Press Limited: London, 1992.
22. Sugiyama, J., personal communication, 1996.
23. Woods, R. J.; Dwek, R. A.; Edge, C. J.; Fraser-Reid, B. J. Phys Chem 1995, 99, 3832.
24. Weiner, S. J.; Kollman, P. A.; Nguyen, D. T.; Case, D. A. J Comput Chem 1986, 7, 230.
25. Glennon, T. M.; Zheng, Y.-J.; Grand, S. M. L.; Shutzberg, B. A.; Kim, M. M., Jr. J Comput Chem 1994, 15, 1019.
26. Ha, S. N.; Giammona, A.; Field, M.; Brady, J. W. Carbohydr Res 1988, 180, 207.
27. Brown, D.; Neyertz, S. Mol Phys 1995, 84, 577.
28. Brown, D. The gmq User Manual, 1999.
29. Rappé, A. K.; Casewit, C. J.; Colwell, K. S.; Goddard, III, W. A.; Skiff, W. M. J Am Chem Soc 1992, 114, 10024.
30. Horii, F.; Yamamoto, H.; Kitamaru, R.; Tanahashi, M.; Higuchi, T. Macromolecules 1987, 20, 2946.
31. Yamamoto, H.; Horii, F.; Odani, H. Macromolecules 1989, 22, 4130.
32. Blackwell, J.; Vasko, P. D.; Koenig, J. L. J Appl Phys 1970, 41, 4375.
33. Aabloo, A. Ph.D. Thesis, Tartu University, Estonia, 1994.
34. Sugiyama, J.; Persson, J.; Chanzy, H. Macromolecules 1991, 24, 2461.
35. Michell, A. J. Carbohydr Res 1993, 241, 47.
36. Brown, D.; Clarke, J. H. R. Macromolecules 1991, 24, 2075.
37. Tashiro, K.; Kobayashi, M. Polymer 1996, 37, 1775.
38. Tashiro, K.; Kobayashi, M. Polymer 1991, 32, 1516.